Technical Notes

TECHNICAL NOTES are short manuscripts describing new developments or important results of a preliminary nature. These Notes cannot exceed 6 manuscript pages and 3 figures; a page of text may be substituted for a figure and vice versa. After informal review by the editors, they may be published within a few months of the date of receipt. Style requirements are the same as for regular contributions (see inside back cover).

Dynamic Response of a Diagonal Line-Loaded Rectangular Plate

M. M. Stanišić*
Purdue University, West Lafayette, Ind.

I. Introduction

At the present time, many of the existing methods of analysis in structural mechanics are a direct extension of the methods used in classical plate and shell theory. Most of these methods are approximative in nature, and because of their simplicity in a mathematical sense, they are used widely in engineering. Such methods are the methods of calculus of variations, finite-element method, and many others. Especially in the last decade, the finite-element method has been widely applied in engineering. In many circumstances, engineers apply this method to problems in mathematical physics and applied mechanics without going into the phenomenological structure of the problem under consideration. Moreover, in most cases the proof of convergence of the results obtained by this method is not a trivial task. In addition, it should be pointed out that there are many problems where the approximate solution requires more time than the solution obtained by exact methods. Therefore, whenever it is possible to obtain a solution in "exact" form by means of operational calculus, then corresponding methods should be used. "Exact" means that the series solution obtained in a closed form converges rapidly. In this Note the methods of operational calculus instead of, for instance, the finite-element method, will be used in order to determine the dynamic response of a rectangular plate, diagonal line-loaded by an arbitrary forcing function. Such problems as the diagonally loaded plate exist in engineering in supersonic wing theory where the wing is subjected to a shock wave caused by corner effect, or in ship design where the structure can be loaded diagonally by severe waves due to storms. Special cases of loading functions, as illustrative examples, will be considered. The convergence of the solution will be discussed.

II. Problem Statement and its Solution

We consider the problem of a rectangular plate, simply supported along the edges, subjected to a line-load depending on position and time as shown in Fig. 1. It should be pointed out that there is no practical difficulty when other types of boundary conditions are considered. The equation governing the equilibrium of the plate under any arbitrary loading function $q(x,y,t)$ can be written as

$$\nabla^4 w(x,y,t) + \frac{\rho h}{D}\frac{\partial^2 w(x,y,t)}{\partial t^2} = \frac{1}{D} q(x,y,t) \tag{1}$$

where

$$\nabla^4 = \frac{\partial^4}{\partial x^4} + 2\frac{\partial^4}{\partial x^2 \partial y^2} + \frac{\partial^4}{\partial y^4} = \text{biharmonic operator}$$

Received Nov. 23, 1976; revision received June 13, 1977.
Index categories: Aeroelasticity and Hydroelasticity; Structural Design; Structural Dynamics.

*Professor, School of Aeronautics and Astronautics.

D = flexural rigidity of the plate
a,b = lateral dimensions of the plate
h = thickness of the plate material
E = Young's modulus of elasticity
ν = Poisson's ratio
$w(x,y,t)$ = vertical displacement
$q(x,y,t)$ = forcing function

Equation (1) is subjected to the following boundary conditions:

$$w(0,y,t) = 0 \quad \frac{\partial^2 w(0,y,t)}{\partial x^2} = 0 \tag{2a}$$

$$w(a,y,t) = 0 \quad \frac{\partial^2 w(a,y,t)}{\partial x^2} = 0 \tag{2b}$$

$$w(x,0,t) = 0 \quad \frac{\partial^2 w(x,0,t)}{\partial y^2} = 0 \tag{2c}$$

$$w(x,b,t) = 0 \quad \frac{\partial^2 w(x,b,t)}{\partial y^2} = 0 \tag{2d}$$

and the initial conditions are

$$w(x,y,0) = g(x,y), \quad \dot{w}(x,y,0) = k(x,y) \tag{3}$$

where $g(x,y)$ and $k(x,y)$ are given functions and the dot represents the derivative with respect to time. Equations (1-3) define our problem. Furthermore, in our case

$$q(x,y,t) = f(t)P(x,y) \tag{4}$$

where $f(t)$ is a pure function of time only, and $P(x,y)$ is a function representing line loading. Evidently, according to Fig. 1 we have

$$P(x,y) = P_0\left\{H\left[y - \left(\frac{b}{a}x - \epsilon\right)\right] - H\left[y - \left(\frac{b}{a}x + \epsilon\right)\right]\right\} \tag{5}$$

Here, P_0 is the amplitude of the load, ϵ is small displacement, and

$$H\{y - [(b/a)x - \epsilon]\} = \begin{matrix} 1 & y \geq (b/a)x - \epsilon \\ 0 & y < (b/a)x - \epsilon \end{matrix} \tag{6}$$

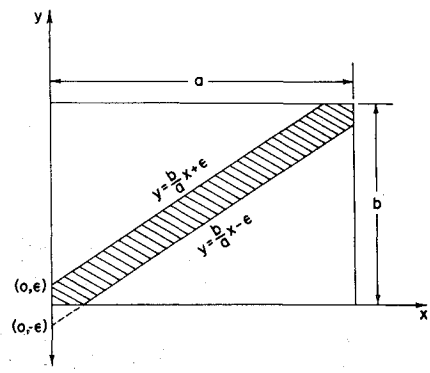

Fig. 1 Geometry of the plate and loading.

$$H\{y-[(b/a)x+\epsilon]\}=\begin{matrix}1\\0\end{matrix}\begin{matrix}\}y\geq(b/a)x+\epsilon\\\}y<(b/a)x+\epsilon\end{matrix} \tag{7}$$

where $H\{\ \}$ denotes a unit step function in the Heaviside sense.

The boundary conditions, Eq. (2), suggest the use of a Fourier-finite sine transform. Namely, we define

$$\omega(n,y,t)=\int_0^a w(x,y,t)\sin\frac{n\pi x}{a}\,dx \tag{8}$$

then,

$$w(x,y,t)=\frac{2}{a}\sum_{n=1}^{\infty}\omega(n,y,t)\sin\frac{n\pi x}{a} \tag{9}$$

Hence, Eqs. (1, 2, and 8) lead to

$$\frac{\partial^4\omega(n,y,t)}{\partial y^4}-2\alpha^2\frac{\partial^2\omega(n,y,t)}{\partial y^2}+\alpha^4\omega(n,y,t)+\frac{1}{C^2}\frac{\partial^2\omega(n,y,t)}{\partial t^2}$$

$$=\frac{1}{D}\int_0^a q(x,y,t)\sin\frac{n\pi x}{a}\,dx \tag{10}$$

where

$$\alpha=(n\pi/a);\quad C^2=D/\rho h \tag{11}$$

Define

$$\Omega(n,m,t)=\int_0^b \omega(n,y,t)\sin\frac{m\pi y}{b}\,dy \tag{12}$$

then,

$$\omega(n,y,t)=\frac{2}{b}\sum_{m=1}^{\infty}\Omega(n,m,t)\sin\frac{m\pi y}{b} \tag{13}$$

Evidently, Eqs. (2, 10, and 12) lead to

$$\frac{\partial^2\Omega(n,m,t)}{\partial t^2}+\lambda^2\Omega(n,m,t)=C^2Q(n,m,t) \tag{14}$$

where

$$\lambda^2=C^2(\alpha^2+\beta^2)^2;\quad \beta=(m\pi/b) \tag{15}$$

with

$$Q(n,m,t)=\frac{1}{D}\int_0^a\int_0^b q(x,y,t)\sin\alpha x\sin\beta y\,dx\,dy \tag{16}$$

In our case

$$Q(n,m,t)=f(t)\frac{P_0}{D}\int_0^a\int_0^b\left\{H\left[y-\left(\frac{b}{a}x-\epsilon\right)\right]\right.$$

$$\left.-H\left[y-\left(\frac{b}{a}x+\epsilon\right)\right]\right\}\cdot\sin\alpha x\,\sin\beta y\,dx\,dy \tag{17}$$

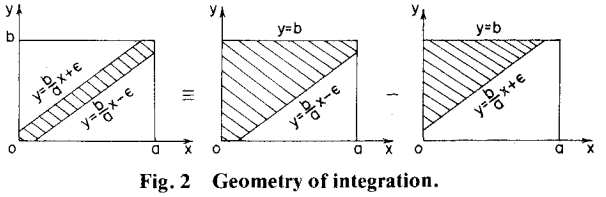

Fig. 2 Geometry of integration.

Now, we integrate Eq. (17) with respect to y first (see Fig. 2), then

$$\int_0^b\left\{H\left[y-\left(\frac{b}{a}x-\epsilon\right)\right]-H\left[y-\left(\frac{b}{a}x+\epsilon\right)\right]\right\}\sin\beta y\,dy$$

$$=\int_{(b/a)x-\epsilon}^{b}\sin\beta y\,dy-\int_{(b/a)x+\epsilon}^{b}\sin\beta y\,dy$$

$$=\left(\frac{2b}{m\pi}\right)\sin\frac{m\pi x}{a}\sin\frac{m\pi\epsilon}{b} \tag{18}$$

Hence, Eqs. (17) and (18) lead to

$$Q(n,m,t)=f(t)\frac{P_0}{D}\frac{2b}{m\pi}\sin\frac{m\pi\epsilon}{b}\int_0^a\sin\frac{m\pi x}{a}\sin\frac{n\pi x}{a}\,dx \tag{19}$$

Note that

$$\int_0^a\sin\frac{m\pi x}{a}\sin\frac{n\pi x}{a}\,dx=\begin{matrix}0\\\frac{a}{2}\end{matrix}\begin{matrix}\}\text{when } m\neq n\\\}\text{when } m=n\end{matrix} \tag{20}$$

Therefore, Eq. (19) by virtue of Eq. (20) becomes

$$Q(n,m,t)=f(t)\frac{P_0}{D}\frac{ab}{m\pi}\sin\frac{m\pi\epsilon}{b} \tag{21}$$

Equation (21) can be written as

$$Q(n,m,t)=f(t)\frac{P_0}{D}ab\left(\frac{\epsilon}{b}\right)\frac{\sin(m\pi\epsilon/b)}{(m\pi\epsilon/b)} \tag{22}$$

since ϵ is small, then $[\sin(m\pi\epsilon/b)/(m\pi\epsilon/b)]\to 1$, so that

$$Q(n,m,t)=f(t)\frac{P_0}{D}ab\left(\frac{\epsilon}{b}\right) \tag{23}$$

Hence, by means of Laplace transform with respect to t, the solution of Eq. (14) becomes,

$$\Omega(n,m,t)=\Omega(n,m,0)\cos\lambda t+\frac{\dot\Omega(n,m,0)}{\lambda}\sin\lambda t$$

$$+\frac{P_0}{D}\frac{abC^2}{\lambda}\left(\frac{\epsilon}{b}\right)\int_0^t f(\tau)\sin\lambda(t-\tau)\,dr \tag{24}$$

Evidently, for any given functions $g(x,y)$ and $k(x,y)$ we find $\Omega(n,m,0)$ and $\dot\Omega(n,m,0)$. Therefore, Eqs. (9) and (13) lead to

$$w(x,y,t)=\frac{4}{ab}\sum_{n=1}^{\infty}\sum_{m=1}^{\infty}\Omega(n,m,t)\sin\alpha x\,\sin\beta y \tag{25}$$

Or, Eq. (25) by means of Eq. (24) results in

$$w(x,y,t)=\frac{4}{ab}\sum_{n=1}^{\infty}\sum_{m=1}^{\infty}\left\{\left[\int_0^a\int_0^b g(x,y)\sin\alpha x\sin\beta y\,dx\,dy\right]\right.$$

$$\times\cos\lambda t+\frac{1}{\lambda}\left[\int_0^a\int_0^b k(x,y)\sin\alpha x\sin\beta y\,dx\,dy\right]\sin\lambda t$$

$$\left.+\frac{P_0}{D}\frac{abC^2}{\lambda}\left(\frac{\epsilon}{b}\right)\int_0^t f(\tau)\sin\lambda(t-\tau)\,d\tau\right\}\sin\alpha x\,\sin\beta y \tag{26}$$

Taking the initial conditions to be zero, then Eq. (26) reduces to

$$w(x,y,t)=\frac{4P_0}{\sqrt{D\rho h}}\left(\frac{\epsilon}{b}\right)\sum_{n=1}^{\infty}\sum_{m=1}^{\infty}\frac{\sin\alpha x\,\sin\beta y}{[\alpha^2+\beta^2]}\times\int_0^t f(\tau)\sin\lambda(t-\tau)\,d\tau \tag{27}$$

This is the solution for the deflection of the plate $w(x,y,t)$ in closed form, for any loading function $f(t)$. We note that $x/a<1$ and $y/b<1$. Hence, the series given by Eq. (27) converges very fast with respect to both integers m and n and any function $f(t)$.

The bending moments in x and y directions are given by

$$M_x(x,y,t)=4P_0\left(\frac{\epsilon}{b}\right)\sqrt{\frac{D}{\rho h}}\sum_{n=1}^{\infty}\sum_{m=1}^{\infty}\frac{[\alpha^2+\nu\beta^2]}{[\alpha^2+\beta^2]}\sin\alpha x\times\sin\beta y\int_0^t f(\tau)\sin\lambda(t-\tau)\,d\tau \tag{28}$$

$$M_y(x,y,t)=4P_0\left(\frac{\epsilon}{b}\right)\sqrt{\frac{D}{\rho h}}\sum_{n=1}^{\infty}\sum_{m=1}^{\infty}\frac{[\nu\alpha^2+\beta^2]}{[\alpha^2+\beta^2]}\sin\alpha x\times\sin\beta y\int_0^t f(\tau)\sin\lambda(t-\tau)\,d\tau \tag{29}$$

Note that $(\alpha^2+\nu\beta^2)<(\alpha^2+\beta^2)$; $(\nu\alpha^2+\beta^2)<(\alpha^2+\beta^2)$. Hence, the convergence of M_x and M_y is evident.

III. Special Examples

A. Case 1

Let

$$f(t)=\cos\gamma t \tag{30}$$

where γ is the driving frequency. Then,

$$\int_0^t f(\tau)\sin\lambda(t-\tau)\,d\tau=\sin\lambda t\int_0^t\cos\lambda\tau\cos\gamma\tau\,d\tau-\cos\lambda t\int_0^t\sin\lambda\tau\cos\gamma\tau\,d\tau \tag{31}$$

Note that

$$\int\cos ax\,\cos bx=\frac{\sin(a-b)x}{2(a-b)}+\frac{\sin(a+b)x}{2(a+b)}\quad\text{for }(|a|\neq|b|) \tag{32a}$$

$$\int\sin ax\,\cos bx=\frac{\cos(a+b)x}{2(a+b)}-\frac{\cos(b-a)x}{2(a-b)}\quad\text{for }(a^2\neq b^2) \tag{32b}$$

Hence, Eqs. (31) and (32) lead to

$$\int_0^t\cos\gamma\tau\sin\lambda(t-\tau)\,d\tau=\frac{\lambda}{\lambda^2-\gamma^2}(\cos\gamma t-\cos\lambda t) \tag{33}$$

Therefore, Eq. (27) becomes

$$w(x,y,t)=\frac{4P_0}{\rho h}\left(\frac{\epsilon}{b}\right)\sum_{n=1}^{\infty}\sum_{m=1}^{\infty}\frac{\cos\gamma t-\cos\lambda t}{\lambda^2-\gamma^2}\sin\alpha x\,\sin\beta y \tag{34}$$

However, since

$$\lambda^2=C^2(\alpha^2+\beta^2)^2$$

then, Eq. (34) converges very fast, for $\lambda^2\neq\gamma^2$. Equation (34) can be written as

$$\frac{w(x,y,t)}{(4P_0/\rho h)(\epsilon/b)}=\sum_{n=1}^{\infty}\sum_{m=1}^{\infty}\frac{\cos\gamma t-\cos\lambda t}{\lambda^2-\gamma^2}\sin\alpha x\,\sin\beta y \tag{35}$$

Evaluation of Eq. (35) for a given geometry of the plate, a and b, and for a given load, ϵ, P_0, and γ, can be evaluated with a slide rule very quickly. However, the application of a finite-element method in the dynamic case requires the solution under a specific load at a given magnitude of the load.

B. Case 2

$$f(t)=e^{-\kappa t} \tag{36}$$

where κ is the driving frequency. Hence, Eq. (36) leads to

$$\int_0^t f(\tau)\sin\lambda(t-\tau)\,d\tau=\sin\lambda t\int_0^t e^{-\kappa\tau}\cos\lambda\tau\,d\tau-\cos\lambda t\int_0^t e^{-\kappa\tau}\sin\lambda\tau\,d\tau \tag{37}$$

Note that

$$\int e^{ax}\cos bx\,dx=\frac{e^{ax}}{a^2+b^2}(a\cos bx+b\sin bx) \tag{38a}$$

$$\int e^{ax}\sin bx\,dx=\frac{e^{ax}}{a^2+b^2}(a\sin bx-b\cos bx) \tag{38b}$$

Therefore,

$$\int_0^t e^{-\kappa\tau}\sin\lambda(t-\tau)\,d\tau=\frac{1}{\lambda^2+\kappa^2}[\lambda e^{-\kappa t}+\kappa\sin\lambda t-\lambda\cos\lambda t] \tag{39}$$

Hence,

$$w(x,y,t)=\frac{4P_0}{\sqrt{D\rho h}}\left(\frac{\epsilon}{b}\right)\sum_{n=1}^{\infty}\sum_{m=1}^{\infty}\frac{\lambda e^{-\kappa t}+\kappa\sin\lambda t-\lambda\cos\lambda t}{\lambda^2+\kappa^2}\times\frac{\sin\alpha x\sin\beta y}{\alpha^2+\beta^2} \tag{40}$$

The convergence of the solution given by Eq. (40) is evident. Note, for the purpose of quick calculation Eq. (40) can be written, similar to Eq. (35), i.e.,

$$\frac{w(x,y,t)}{(4P_0/\sqrt{D\rho h})(\epsilon/b)}=\sum_{n=1}^{\infty}\sum_{m=1}^{\infty}\frac{\lambda e^{-\kappa t}+\kappa\sin\lambda t-\lambda\cos\lambda t}{\lambda^2+\kappa^2}\times\frac{\sin\alpha x\sin\beta y}{(\alpha^2+\beta^2)} \tag{41}$$

From this analysis it can be seen from Eqs. (27-29) that the deflection and moments, and therefore, the stresses, can be found very easily in a simple form by any practical engineer working in the field, with a hand calculator. Hence, such problems can be solved without using, for instance, the finite-element method, which is used so much, even if it is not necessary, by engineers in practice, and which is costly in time and money. However, there is an old Latin saying: "Ab abusu ad usum non valet consequentia." ("The abuse of a thing is no argument against its proper use.")

IV. Conclusion

The problem of response of a rectangular plate subjected to a diagonal line-load which is, in addition, a function of time has been obtained in closed form by means of operational calculus. The results for the deflection and the moments are given in a simple form such that they can be used by any engineer working in the field without any practical difficulty. Two examples are presented to illustrate the theory. The rapid convergence of the solution has been indicated.

Effect of Lithium and Ammonium Fluorides on Ammonium Perchlorate Decomposition

S.R. Jain,* K.C. Patil,† and V.R. Pai Verneker‡
Indian Institute of Science, Bangalore, India

Introduction

THE importance of the thermal decomposition studies on ammonium perchlorate (AP) using metal oxides and fluorides as additives originates mainly from the fact that these additives are used to modify the burning rates of AP-based solid composite propellants. Recently, we reported the catalytic effect of some metal perchlorate ammines on the thermal decomposition of AP.[1,2] It was noticed that the metal oxides catalyze the AP decomposition by forming the metal perchlorate ammines as intermediates. No thermal decomposition study on AP appears to have been made using the metal fluorides as additives, although lithium fluoride has been reported to be acting as a burning rate retardant when used as an additive to AP-based propellants.[3-5] Similarly, ammonium and lithium fluorides appear to have a significant effect in inhibiting the burning rate of AP.[6-10] It is therefore interesting to examine the effect of these fluorides on AP decomposition.

Experimental

Lithium fluoride and ammonium fluoride were available commercially (National Fluorine Corporation, India) and were used as such. Ammonium perchlorate (Fluka AG, 99.5% purity) was used after recrystallization. Differential thermal analysis (DTA) and thermogravimetric (TG) analysis were carried out in air using platinum cups as sample holders. The heating rates employed were 12 deg/min and 5 deg/min in the case of DTA and TG, respectively. LiF:AP (1:10) and NH_4F: AP (1:10) mixtures (by weight) were prepared and used on the same day.

Results and Discussion

LiF: AP System

The DTA of pure AP shows an endotherm peaking at 240°C due to phase transformation and two exotherms at 300 and 390°C due to decomposition. Under identical conditions, the DTA curve of AP remains virtually unchanged when LiF is added to it in a 1:10 weight ratio. This shows apparently no chemical reaction between LiF and AP. However, the isothermal TG of the mixture show interesting behavior (Fig. 1). In the low temperature region, i.e., at 270°C, AP decomposes to about 25% before reaching saturation, whereas in presence of LiF an apparent desensitization of decomposition is observed. At higher temperatures, although AP decomposition is suppressed initially upon addition of LiF, it decomposes rapidly after an induction period. This induction period decreases as the temperature increases. For example, the induction period at 295°C is 200 min, while at 348°C it is only 10 min. The analysis of the residue left behind at the end of the runs showed the presence of lithium perchlorate.

Isothermal TG of $LiClO_4$:AP (1:1) mixture at 295°C showed rapid decomposition of AP without any induction period. A behavior similar to 10% concentration of LiF was observed when lower concentrations, viz, 1, 2, and 5% were used.

This strange effect of LiF on AP decomposition – essentially inactive in dynamic heating conditions but exhibiting activity under isothermal conditions – is essentially due to the fact that longer time is needed for the reaction to occur between the fluoride and AP, which may take place as postulated earlier[5,7,9]:

$$LiF + NH_4ClO_4 \rightarrow LiClO_4 + NH_4F \quad (1)$$

The lithium perchlorate thus formed appears to catalyze AP decomposition at higher temperatures. It is reported[11,12] that the $LiClO_4$:AP system forms a eutectic mixture, melting at 182°C, which is known to catalyze the AP decomposition. The observed catalytic activity at 290°C and above may therefore be due to the eutectic formation. The formation of lithium perchlorate in the LiF:AP system was confirmed by heating a mixture of LiF:AP (1:1 mole ratio) at 295°C for 10 hr. The product (melt) was highly hygroscopic, soluble in water, and gave positive tests for Li^+ and ClO_4^- ions. Further, as can be seen from Fig. 1, the isotherms showed a break at about 14% decomposition, before the onset of rapid decomposition. When the runs were interrupted at this point (14%), melt formation was observed in all cases.

In order to explain the apparent desensitization of AP up to 14% decomposition in presence of LiF, the effect of other, analogous additives, e.g., NaF, MgF_2, on AP decomposition was studied. The DTA of NaF:AP (1:10) and MgF_2:AP (1:10) mixtures under identical conditions did not show any catalysis, i.e., there was hardly any change in the ignition temperatures of AP. But isothermal TG curves (Fig. 2) of the mixtures at 270°C showed suppression in the decomposition of AP, similar to LiF. However, there was no catalysis of AP

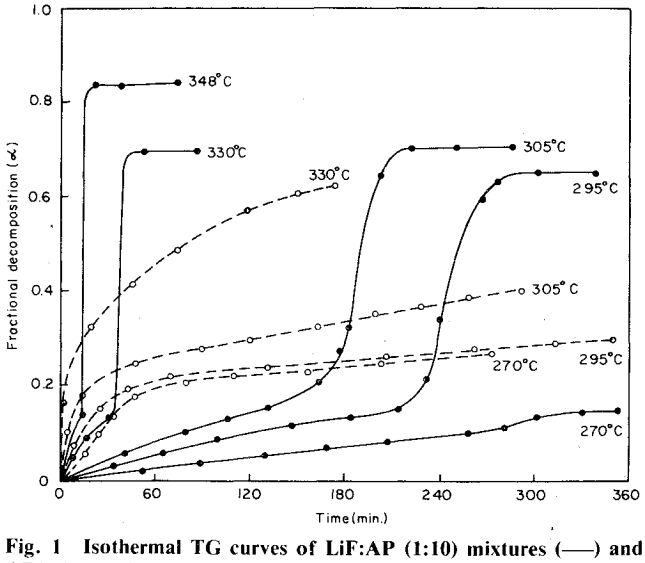

Fig. 1 Isothermal TG curves of LiF:AP (1:10) mixtures (——) and AP(---) at various temperatures.

Received Dec. 20, 1976; revision received Aug. 29, 1977.
Index categories: Fuels and Propellants, Properties of; Thermochemistry and Chemical Kinetics.

*Associate Professor, Department of Aeronautical Engineering.
†University Grants Commission Research Associate, Department of Inorganic and Physical Chemistry.
‡Professor, Department of Inorganic and Physical Chemistry.